

Neural mechanisms in processing of emotion in real and virtual faces

A functional near-infrared spectroscopy (fNIRS) study

Dylan Rapanan

March 3, 2025

Task Paradigm

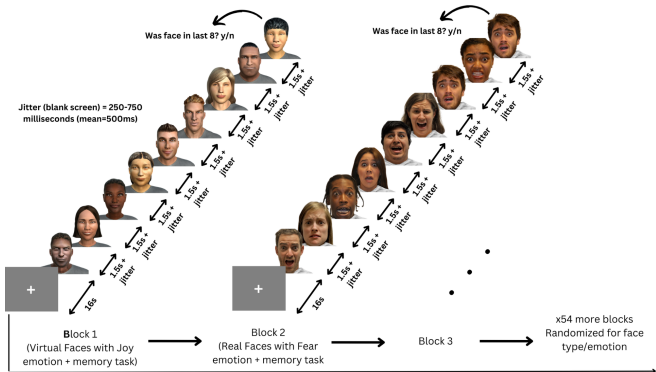


Figure 1: Participants viewed 56 blocks of 8 faces (4 male, 4 female) from two sets: real (RADIATE) and virtual (UIBVFED). Each face displayed one of 7 emotions (anger, disgust, fear, happiness, sadness, surprise, neutral)

fNIRS Montage

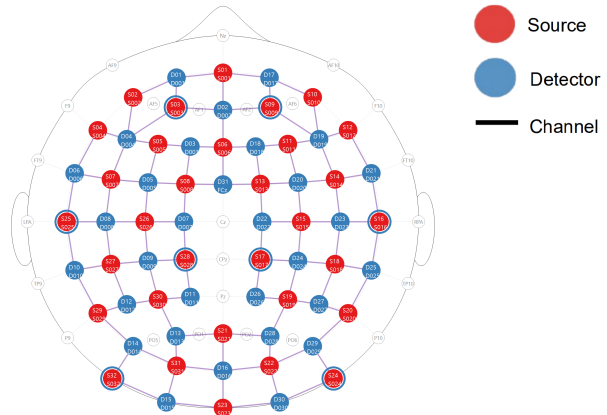


Figure 2: High density 32x32 fNIRS probe layout with 206 channels. fNIRS data recorded using two NIRS Sport2 systems with sampling rate: 6.105 Hz at wavelengths: 760 nm and 850 nm.

Signal Quality

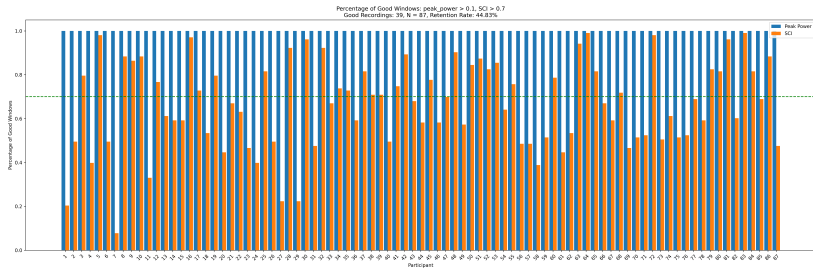


Figure 3: Peak power < 0.1 and the Scalp Coupling Index (SCI) < 0.7 were calculated for 5s sliding windows for each channel for each participant. The dotted green line represents the 70% threshold for good windows.

- ▶ If > 70% of the windows in a channel were good, the channel was deemed good.
- ▶ If > 70% of the channels in a participant were good, the participant was deemed good.
- ▶ Out of 87 participants, 39 are currently deemed good.

Signal Quality by Channel

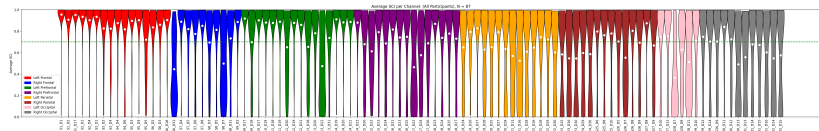


Figure 4: Average SCI for each channel across all participants. The channels are color coded by brain region. The wider the line, the more participants had a SCI value in that range.

- ▶ We can see that the channels towards the back of the head tend to have lower SCI values (this may be because people have lots of hair at the back of their head).
- ▶ There are a select few channels that have low SCI values across all participants.

General Linear Model (GLM) Analysis

► Design Matrix Construction:

- Use a cosine drift model with high-pass filtering (cutoff = 0.03125 Hz; ~32 s period) to remove low-frequency trends.
- Model the haemodynamic response with the Statistical Parametric Mapping (SPM) Haemodynamic Response Function (HRF) over a 16s stimulus duration.

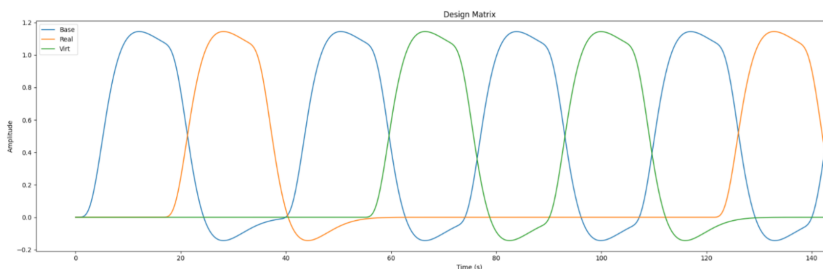


Figure 5: Design matrix for a single participant (first 150s). Each condition is represented by a different color and represents the onset of a block.

GLM Analysis

► First-Level GLM:

- Fit GLM per recording to estimate condition-specific responses.
- Extract both channel-level and ROI estimates.

► Group-Level Analysis: $\theta \sim -1 + \text{ROI} : \text{Condition} : \text{Chroma}$

- This mixed effects model estimates separate coefficients (θ 's) for each combination of ROI, condition, and channel type without a global intercept.
- Group by participant for variability between subjects.

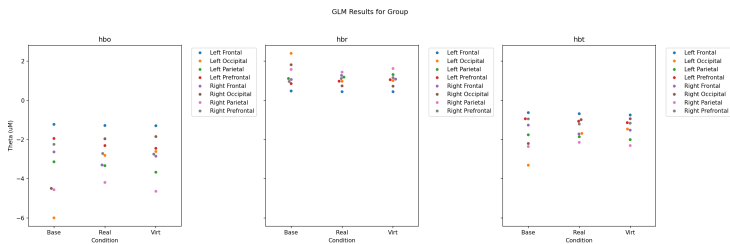


Figure 6: Swarm plots display θ 's across conditions/ROIs for each channel type. Higher θ values indicate stronger responses.

GLM Contrasts

► Contrasts:

- Contrasts between pairs of conditions (i.e. Joy - Fear) are defined by subtracting corresponding regressors.
- This highlights the differences in haemodynamic responses under the combinations of conditions.

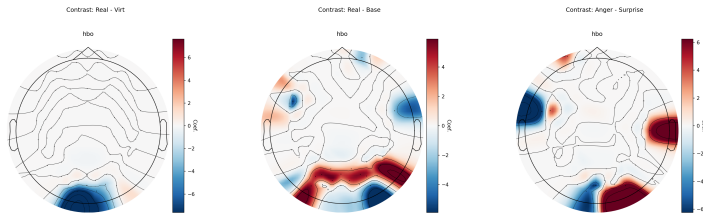


Figure 7: Contrast maps (Hbo) for Real vs. Virtual (left), Real vs. Baseline (middle), and Anger vs. Surprise (right).

- Only channels with $P < |z|$ greater than 0.05 are displayed, indicating a significant difference in Hbo.

Event Related Potentials (ERPs)

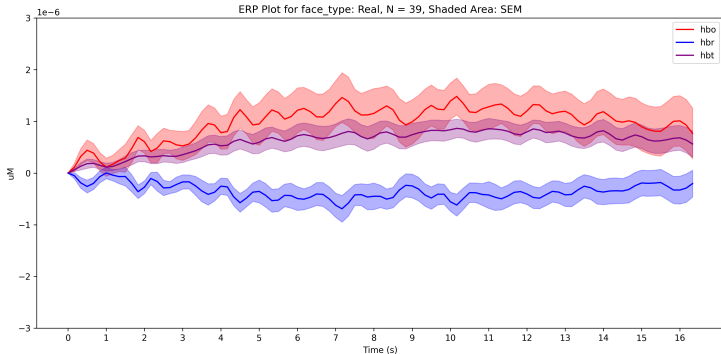


Figure 8: ERP for real face epochs across all channels. The x-axis represents time in seconds (s) and the y-axis represents the $\Delta Hbo/Hbr/Hbt$ in micromolars (μM).

- The shaded region is the standard error of the mean (SEM):
$$\frac{\sigma}{\sqrt{n}}$$
.

ERP Differences

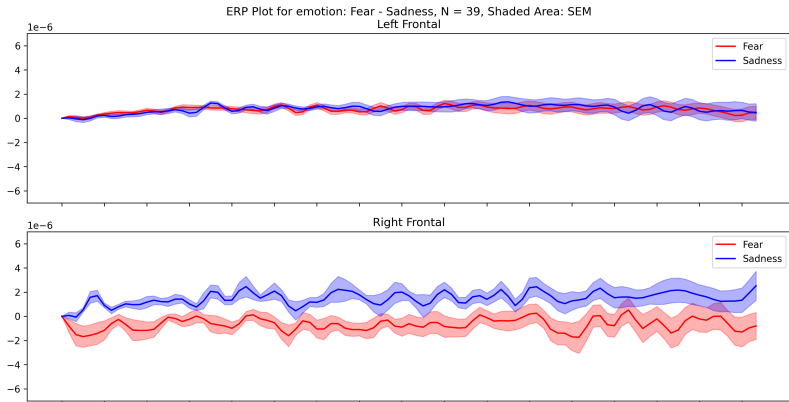


Figure 9: ERP difference in Hbo between fear and sadness for Left/Right frontal regions.

ERP Differences

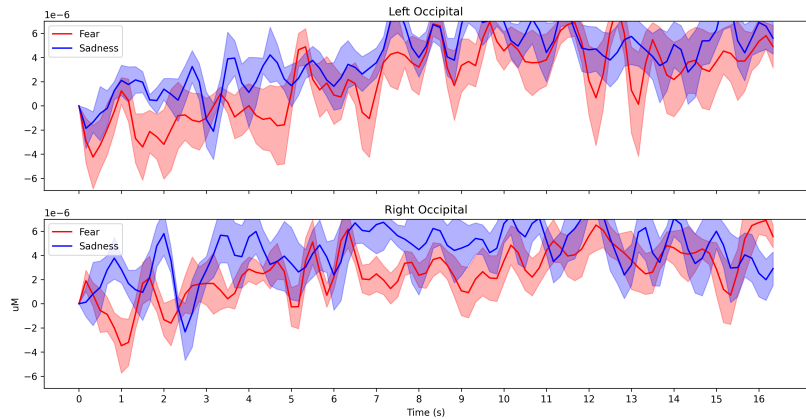


Figure 10: ERP difference in Hbo between fear and sadness for Left/Right occipital regions.

Connectivity Analysis

► Connectivity Analysis:

- Continuous Wavelet Transform with a Morlet wavelet to analyze the frequency-domain characteristics of the data.
- Connectivity matrices were computed resulting in a 5D (num_participants, num_channel_types, num_channel_connections, num_frequencies, num_times) array for each condition.

► Connectivity Parameters:

- `channel_types = ['hbo', 'hbr', 'hbt'] # channel types to analyze`
- `method = "coh" # coherence is used as the connectivity metric`
- `con_mode = "cwt_morlet" # the morlet wavelet is used for the CWT`
- `cwt_freqs = np.linspace(0.01, 0.5, 10) # Pick 10 evenly spaced frequencies between 0.01 and 0.5 Hz`
- `cwt_n_cycles = 10 # Number of cycles for the Morlet wavelet`
- `faverage = True # Average the connectivity matrices across frequencies`

Connectivity Heatmaps

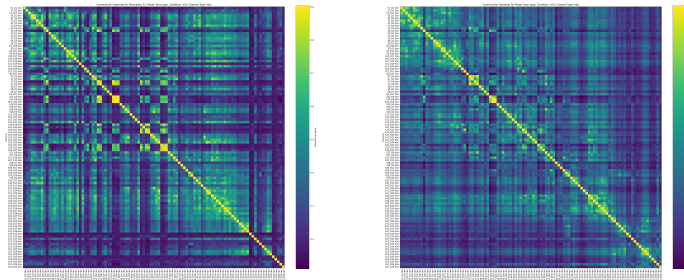


Figure 11: Virtual face connectivity heatmaps for a single participant (left) and the average across all participants (right). The x-axis and y-axis represent the channel number. A brighter color represents higher connectivity strength.

- ▶ We can see that the average connectivity heatmap has a more washed out distribution of connectivity strength.

Connectivity Chord Plots

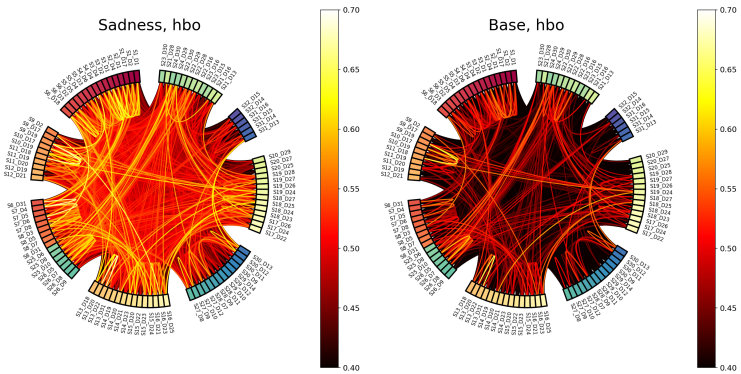


Figure 12: Chord plot of connectivity between channels for sadness (left) and baseline (right) conditions. Brighter lines represent higher connectivity strength.

- ▶ Connections across the middle of the plot indicate connectivity across far apart regions of the brain.

Connectivity Group Level T-Tests Chord Plots

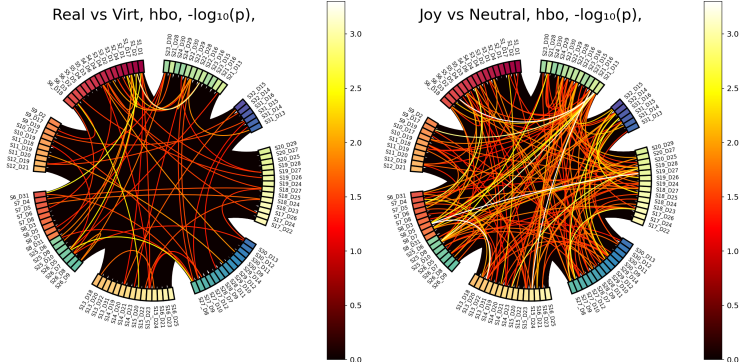


Figure 13: Paired t-tests were conducted on Fisher z -transformed connectivity matrices (reshaped from averaged channel-specific data) for each unique pair of conditions (i.e. Real vs. Virtual (left) and Joy vs. Neutral (right)). p -values were computed for each lower-triangular matrix element across participants and subsequently corrected for multiple comparisons using False Discovery Rate (FDR) correction.

Decoding Analysis

Model Scores for Different Modes (ROC-AUC %)

Model	face_type	emotion
GaussianNB	73.21	56.16
HistGradientBoostingClassifier	81.22	73.3
KNeighborsClassifier	69.75	58.24
LGBMClassifier	81.34	73.39
LogisticRegression	78.17	67.3
MLPClassifier	77.4	65.66
QuadraticDiscriminantAnalysis	51.09	50.15
RandomForestClassifier	83.46	72.36

Figure 14: Spatio-temporal classification performance of multiple machine learning models across conditions. For each model, recordings were preprocessed via scaling and vectorization. The average ROC-AUC scores were computed using five-fold cross-validation over all recordings.